❏ 1882

# Robust super-twisting sliding mode controller for the lateral and longitudinal dynamics of rack steering vehicle

**Norsharimie Mat Adam[1], Addie Irawan[1,2], Mohd Ashraf Ahmad[1]**
[1]Robotics, Intelligent & Control Engineering (RISC) Research Group, Faculty of Electrical & Electronics Engineering Technology, Universiti Malaysia Pahang, Pekan, Pahang, Malaysia
[2]Centre for Automotive Engineering, Universiti Malaysia Pahang, Pekan, Pahang, Malaysia

## Article Info

## ABSTRACT

Inertia phenomenon in steering vehicle is major factor that allow oversteering incident in which come from the insufficient steering and slip control over the vehicle itself. The efficient and robust control system is required to consider both precision and stability of the vehicle for better manuevering especially in cornering road. Therefore, this research has taken the initiative to contribute a better solution for vehicle control according to the mentioned problem and situation with a proposed robust super-twisting sliding mode control (ST-SMC) by simplified torque on wheel and steering angle input with decoupling lateral and longitudinal errors. This control technique approach to allow coping with the issue by reducing forces and inertia for optimum speed at the cornering period and with the almost precise steering positioning. The dynamic model of rack steering vehicle (RSV) is used as the model plant and the proposed control system is simulated for verification. The results shows that the proposed ST-SMC offers improved performance in terms of speed increase time and vehicle stability that gives impact to the RSV being skidded or collided to any obstacles during cornering period.

## Corresponding Author:

Addie Irawan
Robotics, Intelligent & Control Engineering (RISC) Research Group, Faculty of Electrical & Electronics
Engineering Technology, Universiti Malaysia Pahang
Pekan, Pahang 26600, Malaysia
Email: addieirawan@ump.edu.my

## 1. INTRODUCTION

In vehicle dynamic control design and yet, it is usually difficult to be controlled as reported in [1]. Oversteering that causes by the friction forces on the wheel of the vehicle providing inertia generation that disturbing a lot in vehicle handling and operation. The situation is obvious in standard driving vehicle design with the rack steering configuration, whereby this vehicle having a crucial situation in handling inertia especially at the cornering and confined area. Active steering system (ASS) or active front steering system (AFS) in [2], [3] is a popular rack steering vehicle (RSV) setup that is susceptible to inertial effects because to its non-skid arrangement. However, this vehicle is vulnerable to the collisions with the wall or off-road incidents, particularly on cornering tracks, as a consequence of overdriven [4]-[6]. The situation may become worse when this vehicle needs to pass through the uneven terrain and slippery terrain [7]. When the car is oversteered, the RSV mechanisms and the vehicle's transverse axis transform circular motion to linear motion. At high velocities, counter phase steering is incapable of reducing the vehicle's turning radius. Due to the fact that a hard turn might approach the vehicle's minimum turning radius, an accident may occur.

On the other hand, collision and off-road problems for the non-holonomic vehicle such as RSV and other underactuated vehicles are very crucial issues especially when involving safety for driver at the cornering road [8]. This incident happen whenever a vehicle is unable to deal with forces, inertia, as well as vibration during maneuvering especially on the rough and uneven terrain [9], [10]. Moreover, the incident also give impact to the peer's vehicles especially when vehicle at the high-speed level. The basic vehicle automatic control unit facing a serious structural obstruction and lead to unsatisfactory transient performances especially high slip situation at the cornering road. Inertia factor will decrease vehicle stability level and the precision of vehicle path tracking. In addition, at high-speed level the kinetic energy will increased and make event more in the high response states. According to the previous works such as reported in [11], [12], major works were done on the steering precision that emphasized on the body orientation and stability instead of focus on potential and kinetic energy of the vehicle. Therefore, there is restricted research for steering systems satisfying non-integrable kinematics relations [13] with an extension to the underactuated mechanical systems that had non-integrable dynamics (realizing the kinodynamic planning) to reduce inertia through its energy. Several works such as reported in [9], [10], [14] had ocused on yaw angle component of steering vehicle to overcome the lateral force saturation of rear wheel and major vehicle side slip angle that also regarding the vehicle body orientation and stability.

In terms of dynamics and control, the inertia cause by the friction force can be estimated and the longitudinal motion has potential to be controlled through direct actuation of the driving motors [6], [15]. At this point, the new challenge is opened in realizing mentioned proposal when the stiffness on tire motion frequently large in cornering motion. This issue has increased the lateral forces sensitivity toward vehicle states such as steering angle, lateral velocity, and orientation of the vehicle. Moreover, accident may become worse when involving external disturbances from environment such as unstructured and slippery terrain. In previous works, many different control system design approaches have been proposed to deal with uncertainty and disturbance, including computed torque control [16], adaptive control [17], pid control [18], sliding mode control [19], optimal control [20], or different control systems [21]. In general, they've employed SMC to RSV system. In this case, they proposed minimizing the impact of unknown components to a certain range of values. Because of its high resilience, practicality, and simplicity in design, SMC has been commonly implemented to cope with uncertainty and disturbance in systems. Previous studies have summarized the theoretical and practical development of the SMC approach in order to resolve a large amount of uncertainty and disturbance. However, SMC does not guarantee a steady convergence time when faced with quickly fluctuating disturbances and has a weaker transient responsiveness than other approaches when presented with rapidly changing disturbances. As a results, most of the researchers came out with the adaptive and improvement approach to enhance the function of conventional SMC such as done in [22], [23]. Several approaches, such as terminal sliding mode control (T-SMC) [24] and nonsingular fast terminal SMC (NFT-SMC) [23] have been developed to provide finite-time convergence while simultaneously enhancing the dynamic system's convergence features. When the state error variables are far from the equilibrium point, NFT-SMC converges faster than T-SMC.

Hence, this research has taken the initiative to investigate and present an alternate technique that applies both the SMC and super twisting theorem approaches to overcome the side-slipped issue on the RSV system. The proposed solution is emphasized on both inertia and kinetic energy of the vehicle that cause oversteering problem through the analysis on the force tracking performances of the vehicle axial motion. The rest of this research paper is organized as follows. Section 2 describes the problem formulation through the mathematical dynamic modeling of the RSV. For the section 3, details on the proposed robust super twisting sliding mode method (ST-SMC) for RSV control, starting from simplified torque on wheel and steering angle continues to application of ST-SMC control design to the lateral and longitudinal. For the section 4, shows the simulation results of the comparison SMC and ST-SMC system with the presence of external disturbance and finally, section 5 contains the conclusion of the paper.

## 2. PROBLEM FORMULATION AND DYNAMIC MODEL SIMPLIFICATION

At this stage, the RSV model properties are used to achieve the control objectives. Here, the model is simplified from (1) to (3). The vehicle's dynamic model is simplified by employing Euler-Lagrange dynamics, which reduces the number of variables. This formulation simplification was used in order to decrease the number of numerical steps necessary for the symbolic representations of the dynamic model. The dynamical equilibrium of the RSV is simplified as follows.

$$m\ddot{x} - m\dot{\psi}\dot{y} + L_3\dot{\psi}^2 + F_{aero} + F_{ax} = 0 \tag{1}$$

$$m\ddot{y} - m\dot{\psi}\dot{x} + L_3\ddot{\psi} + F_{ay} = 0 \tag{2}$$

$$I_3\ddot{\psi} - L_3\ddot{\psi} - L_3\dot{\psi}\dot{x} + F\psi_y = 0 \tag{3}$$

Considered, the vehicle model is subjected to large external forces from the ground and its tyres. The Dugoff model is used to depict these forces because it is a relevant mix between simplicity and representativity. Notably, the lateral and longitudinal forces, the friction coefficient, the adhesion and stiffness of the wheels, the slip ratio, and the vertical forces are all taken into consideration. The longitudinal aerodynamic forces ($F_{aero}$) is also taken into account as its effect can't be neglected for high speeds. The terms in $L_3$ and $I_3$ in the vehicle model, according to the (3), show the link between the different bodies composing the vehicle. $L_3$ and $I_3$ are defined as in (4) and (5) respectively.

$$L_3 = L_r(m_{rr} + m_{rl}) - L_f(m_{fr} + m_{fl}) \tag{4}$$

$$I_3 = I_z + t_f{}^2(m_{rr} + m_{rl} + m_{fr} + m_{fl}) + L_f{}^2(m_{fr} + m_{fl}) + L_r{}^2(m_{rr} + m_{rl}) \tag{5}$$

According to the (5), the parameters $m$ and $I_z$ represent the vehicle mass and the inertia's moment around the $z$ - axis, $m_{ij}$ is wheel's mass, $L_f$ and $L_r$ are the distances between the COG which front and the rear axles respectively. On the RSV's system, Dugoff's model is utilized $Fx$ and $Fy$ to calculate $E$, the vehicle track.

$$F_{ax} = -cos(\delta_{fl})Fx_{fl} - cos(\delta_{fl})Fx_{fr} - Fx_{rl} - Fx_{rr} + sin(\delta_{fl})Fy_{fl} + sin(\delta_{rl})Fy_{fr} \tag{6}$$

$$F_{ay} = -sin(\delta_{fl})Fx_{fl} - sin(\delta_{fr})Fx_{fr} - cos(\delta_{fl})Fy_{fl} - cos(\delta_{fr})Fy_{fr} - Fy_{rl} - Fy_{rr} \tag{7}$$

$$F_{\psi x} = (-L_f sin(\delta_{fl}) + \frac{E}{2}cos(\delta_{fl}))Fx_{fl} + (-L_f sin(\delta_{fr}) - \frac{E}{2}cos(\delta_{fr}))Fx_{fr} + \frac{E}{2}Fx_{rl} - \frac{E}{2}Fx_{rr} \tag{8}$$

$$F_{\psi y} = (-L_f cos(\delta_{fl}) - \frac{E}{2}sin(\delta_{fl}))Fy_{fl} + (-L_f cos(\delta_{fr}) - \frac{E}{2}sin(\delta_{fr}))Fy_{fr} + L_rFy_{rl} - L_rFy_{rr} \tag{9}$$

Moreover, front wheels are underactuated in which $\tau_{fl} = 0$, $\tau_{fr} = 0$, thus, the torques of RSV can be expressed as in (10). Furthermore, the linear model is used to estimate the between force and the ground in which can be written as (11) and (12) as follows. Note that, $Fx_{ij}$ and $Fy_{ij}$ here are the longitudinal and the lateral forces developed on the four wheels.

$$\tau = \tau_{rl} + \tau_{rr} \tag{10}$$

$$Fx_{ij} = C_{\sigma ij}\sigma_{xij} \tag{11}$$

$$Fy_{ij} = C_{\alpha ij}\alpha_{xij} \tag{12}$$

where $ij$ is the wheel index, $i$ stands for front or rear and stands for left or right. On the other hand, $C_{\sigma ij}$ is longitudinal stiffness of tire, $\sigma_{xij}$ is the longitudinal slip ratio, $C_{\alpha ij}$ is cornering stiffness of tire, and $\alpha_{xij}$ is slip angle of each tire. Note that, the front left and the front right wheel's steering angles are assumed to be equal since the input is from a single steering of the RSV that can be expressed with $\delta_{fl} = \delta_{fr} = \delta$. Let's assumed that.

$$r\omega_{ij} = \dot{x} \tag{13}$$

Where $\omega_{ij}$ is a wheel angular velocity. Thus, the wheel dynamics equations can be written as (14) as follows.

$$I_\omega\omega_{ij} = \tau_{ij} - rFx_{ij} \tag{14}$$

According to the (14), $I_\omega$ is the rotation's moment of inertia and $\tau_{ij}$ is braking and driving torque applied to the RSV's four wheels. Therefore, the longitudinal stiffness of tire can be expressed by substituted (29) and (30) into the (27) as follows.

$$C_{\sigma ij} = \frac{\omega_{ij}}{\dot{x}\sigma_{xij}}(\tau_{ij} - I_\omega\omega_{ij}) \tag{15}$$

On the other hand, by integrating (10) and (15) into (1), it can be obtained that:

$$m\ddot{x} - m\dot{\psi}\dot{y} + L_3\dot{\psi}^2 + F_{aero} - \frac{\tau_{ij}}{R_{eff}} + 4\frac{I_\omega\ddot{x}}{R_{eff}^2} + \delta(F_{yl} + F_{yr}) = 0 \tag{16}$$

whereas (16) indicates the wheels dynamics equations can be reduced by directly relating longitudinal acceleration to the wheels torque. By assuming $C_{af} = C_{afl} = C_{afr}$ and $C_{ar} = C_{arl} = C_{arr}$, the overall simplified vehicle dynamic model can be rewritten as in (17) to (19) as follow:

$$m_e\ddot{x} - m\dot{\psi}\dot{y} + L_3\dot{\psi}^2 + F_{aero} + \delta(2C_{\alpha f}\delta - 2C_{\alpha f}\frac{\dot{x}(\dot{y}-L_f\dot{\psi})}{\dot{x}^2-(\frac{E}{2}\dot{\psi})^2}) = g_1 \tag{17}$$

$$m_e\ddot{y} - m\dot{x}\dot{\psi} + L_3\dot{\psi} + 2C_{\alpha f}\frac{\dot{x}(\dot{y}+L_f\dot{\psi})}{\dot{x}^2-(\frac{E}{2}\dot{\psi})^2}) + 2C_{\alpha r}\frac{\dot{x}(\dot{y}-L_r\dot{\psi})}{\dot{x}^2-(\frac{E}{2}\dot{\psi})^2}) = g_2 \tag{18}$$

$$L_3\ddot{\psi} + 2L_f C_{\alpha f}\frac{\dot{x}(\dot{y}+L_f\dot{\psi})}{\dot{x}^2-(\frac{E}{2}\dot{\psi})^2} - 2L_r C_{\alpha r}\frac{\dot{x}(\dot{y}-L_r\dot{\psi})}{\dot{x}^2-(\frac{E}{2}\dot{\psi})^2} - L_3(\ddot{y} + \dot{x}\dot{\psi}) = g_3 \tag{19}$$

where $m_e$, $g_1$, $g_2$ and $g_3$ are given by as follows:

$$m_e = m + 4\frac{I_\omega}{r} \tag{20}$$

$$g_1 = \frac{\tau\omega_{ij}}{r} \tag{21}$$

$$g_2 = (2C_{\alpha f} - 2\frac{I_\omega}{r^2}\ddot{x})\delta \tag{22}$$

$$g_3 = (L_f g_2 + \frac{E}{2}C_{\alpha f} - \frac{E\dot{\psi}(\dot{y}-L_f\dot{\psi})}{\dot{x}^2-(\frac{E}{2}\dot{\psi})^2}\ddot{x})\delta \tag{23}$$

The simplified model in (17)-(19) is utilized to develop the control laws. Errors between the dynamic variables and their target values must be eliminated in order to achieve the control goal. In other words, the desirable dynamics settle into an equilibrium. When this is acquired, $\dot{x}, \dot{y}, \dot{\psi}$ and $\delta$ are given by (using (17)-(19)) and cancelling the accelerations $\ddot{x}, \ddot{y}$ and $\ddot{\psi}$:

$$\dot{x} \triangleq \dot{x}_{eq} = \dot{x}* \tag{24}$$

$$\dot{\psi} \triangleq \dot{\psi}_{eq} = P_{ref}\dot{x} \tag{25}$$

$$\dot{y} \triangleq \dot{y}_{eq} = L_r\dot{\psi}_{eq} - \frac{mL_f+L_3}{2(L_f+L_r)C_{\alpha f}}\dot{\psi}_{eq}\dot{x}^2 \tag{26}$$

$$\delta \triangleq \delta_{eq} = \frac{(2L_f C_{\alpha f}-2L_r C_{\alpha r})\dot{y}_{eq}+(2L_f C_{\alpha f}-2L_r^2 C_{\alpha r})\dot{\psi}_{eq}-L_3\dot{x}^2\dot{\psi}_{eq}}{2L_f C_{\alpha f}\dot{x}} \tag{27}$$

Noted that, the controller is to ensure robust control of the reference trajectory for any time varying maneuver. Thus, the controller calculates the driving needed to maintain a certain intended speed, and the steering wheel angle that reduces the lateral displacement error with respect to a specific reference trajectory. According to a reference track, the vehicle's center of gravity (COG) error dynamics is shown as follows:

$$\alpha_y* = \dot{x}^2 P_{ref} \tag{28}$$

The vehicle's lateral acceleration along the reference track is represented by $\alpha_y*$. According to (29), the vehicle's lateral acceleration may be described as $\dot{x}^2 P_{ref}$, where $P_{ref}$ is the reference trajectory curvature, and $e_{vx} = \dot{x} - \dot{x}*$ provided that this is the case, (29) can be represented as follows.

$$\ddot{e}_y = \alpha_y - \alpha_y* = \ddot{y} + \dot{x}\dot{\psi} - \dot{x}^2 P_{ref} \tag{29}$$

## 3.    ROBUST SUPER-TWISTING SLIDING MODE FOR VEHICLE SLIP CONTROL

The robust (ST-SMC) classified in two stages of structure: simplified controller input states and control system design. For the simplification of the controller input states, both torque on wheel and steering angle error states are simplified with the proposed decoupling technique. These simplified input states then will be applied on the controller design stage where immersion and invariance control technique are applied. According to the (30), the trajectory is guaranteed if and only if $s_1$ and $s_2$ converge asymptotically to zero. The aim is to achieve that:

$$\lim_{t \to +\infty} s_1 = \lim_{t \to +\infty} \dot{e}_y = \lim_{t \to +\infty} e_y = 0,$$

$$\lim_{t \to +\infty} s_2 = \lim_{t \to +\infty} \dot{e}_{vx} = 0 \tag{30}$$

At this stage, the Lyapunov function is used to deduce the suitable control laws. The aim of the design is to provide the algorithm that can cater both the longitudinal and lateral dynamics control for RSV system in parallel. Therefore, the two significant error states are defined as in the (31) and (32) as follows.

$$s_1 = \dot{e}_y \lambda_y e_y, \qquad \lambda_y = 0 \tag{31}$$

$$s_2 = \dot{e}_{vx} \lambda_x \int e_{vx}, \quad \lambda_x = 0 \tag{32}$$

where $s_1$ is a function of the lateral displacement error ($e_y$) and $s_2$ is a function of the vehicle longitudinal differential error. Meanwhile, $\lambda_x$ and $\lambda_y$ are both positive constants. The vector with superscript ($*$) represent desired outputs. Noticed that (1) is taken as an error dynamic at the vehicle's central gravity, with reference to the reference track. The control design is aim for two-in-one step by dealing with both nonlinearities of the longitudinal and lateral dynamics of the vehicle. Thus, the Lyapunov function is used, where $\gamma$ it is a positive parameter and both $s_1$ and $s_2$ are candidates as expressed in (33) and (34) respectively as follows:
Proof. Consider the Lyapunov functions.

$$V = \frac{1}{2}s_1{}^2 + \frac{1}{2}\gamma s_2{}^2, \quad \gamma > 0 \tag{33}$$

$$\dot{V} = s_1 \dot{s}_1 + \gamma s_2 \dot{s}_2 \tag{34}$$

As a result, the convergence of $s_1$ and $s_2$ can guarantees the intersection of $e_y, \dot{e}_y$ and $e_{vx}$. Note that, the negative variation $V$ can be expressed as in (35).

$$\dot{V} = s_1 \dot{s}_1 + \gamma s_2 \dot{s}_2 = -K_{lyy}s_1 - \gamma K_{lyx}s_2{}^2 \tag{35}$$

where $K_{lyy}$ and $K_{lyx}$ are the positive gains of the controller. The condition in (51) can be satisfied by taking (36) and (37), which yields (38) and (39).

$$s_1 \dot{s}_1 = -K_{lyy}s_1{}^2 \tag{36}$$

$$s_2 \dot{s}_2 = -\gamma K_{lyx}s_2{}^2 \tag{37}$$

$$\dot{s}_1 = K_{lyy}s_1 \tag{38}$$

$$\dot{s}_2 = -\gamma K_{lyx}s_2 \tag{39}$$

Note that, (31) and (32) are used to get (40) and (41) as follows:

$$\dot{s}_1 = \ddot{e}_y + \lambda_y \tag{40}$$

$$\dot{s}_2 = \dot{e}_{vx} + \lambda_x e_{vx} = \ddot{x} - \ddot{x}^* + \lambda_x(\dot{x} - \dot{x}^*) \tag{41}$$

Then, by integrating (40) and (41) into (38) and (39) respectively, (30) and (31) can be obtained as follows:

$$\ddot{e}_y = -(K_{lyy} + \lambda_y)\dot{e}_y - K_{lyy}\lambda_y e_y \tag{42}$$

$$\ddot{x} = \ddot{x}^* - (K_{lyy} + \lambda_x)e_{vx} - K_{lyx}\lambda_x e_{vx} \tag{43}$$

At this stage, by integrating (40) into (42), (44) can be obtained as follows:

$$\ddot{y} = \dot{x}^2 P_{ref} - \dot{x}\dot{\psi}(K_{lyy} + \lambda_y)\dot{e}_y - K_{lyy}\lambda_y e_y \tag{44}$$

As a result, we can determine the longitudinal and lateral control inputs by substituting (45) for (46) in the simplified system. Thus, the output feedbacks of the torque on the wheel and the steering angle can be simplified as follows.

$$e_w = r\left[m_e \ddot{x}^* - m_e(K_{lyx} + \lambda_x)e_{vx} - m_e(K_{lyx}\lambda_x)\int e_{vx} - m\dot{y}\dot{\psi} + L_3\dot{\psi}^2 + \delta(2C_{af}\delta - 2C_{af}\frac{\dot{x}(\dot{y}+L_f\dot{\psi})}{\dot{x}^2-(\frac{E}{2}\dot{\psi})^2}) + F_{aero}\right] \tag{45}$$

$$e_\delta = \frac{1}{2C_{af}-2\frac{I_w}{R_{eff}}\ddot{x}}\left[m\dot{x}^2 P_{ref} - m(K_{lyy} + \lambda_y)\dot{e}_y - L_3\ddot{\psi} + mK_{lyy}\lambda_y e_y + 2C_{af}\frac{\dot{x}(\dot{y}+L_f\dot{\psi})}{\dot{x}^2-(\frac{E}{2}\dot{\psi})^2} + 2C_{ar}\frac{\dot{x}(\dot{y}-L_r\dot{\psi})}{\dot{x}^2-(\frac{E}{2}\dot{\psi})^2}\right] \tag{46}$$

According to (35), $e_y$ it is then replaced by $e_{yf}$ in (46), where $e_y$ is the lateral displacement error computed at the vehicle's COG and $e_\psi$ is the orientation angle regarding the reference trajectory. Noted that the torque computation considers the lateral dynamic, and the steering angle computation includes both longitudinal speed and acceleration. To apply proposed ST-SMC to the RSV, the output of vehicle lateral error state in (46) is used in the design. Therefore, when the super-twisting theorem [25] is applied, the steering angle output of the ST-SMC controller can be written as follows:

$$u_{ST-SMC} = \delta_{ST} + \delta_{eq} \tag{47}$$

where $u_{ST-SMC}$ is the super twisting algorithm given by:

$$\delta_{ST} = z_1 + z_2 \tag{48}$$

$$z_1 = -\alpha|s_1|^{\frac{1}{2}}sign(s_1) \tag{49}$$

$$z_2 = -\beta sign(s_1) \tag{50}$$

$$\delta_{eq} = \frac{1}{2C_{af}-2\frac{I_w}{r^2}\ddot{x}}\left[L_3\ddot{\psi} - 2C_{af}\frac{\dot{x}(\dot{y}+L_f\dot{\psi})}{\dot{x}^2-(\frac{E}{2}\dot{\psi})^2} - 2C_{ar}\frac{\dot{x}(\dot{y}-L_r\dot{\psi})}{\dot{x}^2-(\frac{E}{2}\dot{\psi})^2} - \dot{x}^2 P_{ref} + \lambda e_y\right] \tag{51}$$

Noted that, $\alpha$ and $\beta$ in the (49) and (50) are the positive constants from the model RSV. As a result, the proposed ST-SMC system can be assured of its stability going forward. The complete control system architecture for RSV with the proposed ST-SMC is presented in Figure 1 by utilizing (51) in order to define the control input design.
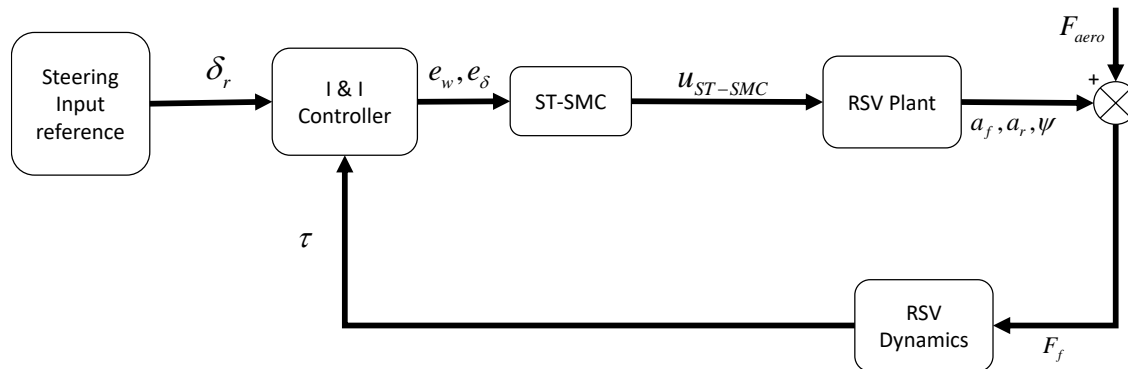


Figure 1. The overall control architecture of proposed ST-SMC on RSV system

## 4. RESULTS AND DISCUSSION

According to Figure 2, a discrete trajectory waypoint for the *X–Y* position was used as input to the simulation model for simulation and analysis. To assess the performance of RSV in cornering period, the trajectory has been taken from the local frame coordinate data (*X–Y* position). The simulation aimed to simulate the vehicle cornering by influencing the cornering angles of the vehicle. The angle of RSV for the cornering of c-shape cornering was set about 86°. Simulated tests under various conditions are utilized to evaluate the proposed ST-SMC approach and compare it to prior studies that employed SMC. To implement the proposed robust control strategy with ST-SMC in the system, parameters such as the trajectory, steering angle and lateral and longitudinal vehicle error were used and likely drawn from the RSV model. Since the vehicle is understeer in a cornering line on the road, it is assumed that it is travelling understeer. Initially, the slip of the RSV with existing SMC and ST-SMC was compared by considering a completely empty vehicle with a $\mu_{max}$ of 0.8 on the road surface. Since this research considers the RSV system, the total braking force of the rear wheels during braking wheels are shared through regenerative braking and friction braking, while the front wheels always only perform friction braking. As shown in Figure 2, RSV without a controller appears to be very unstable (for the longitudinal and lateral) in the presence of disturbances such as rolling resistance, air-wind, and friction force, which have been added in simulation. The situation gets stable with no jerky and low oscillation on path motion when controller was applied. SMC shows eliminating the jerky in RSV path motion but having a problem in tracking error as compared to the ST-SMC.
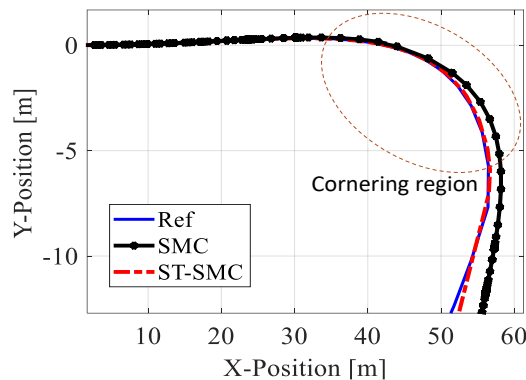


Figure 2. Trajectory and path planning performances between proposed ST-SMC and SMC for the c-shape cornering

As seen in the Figure 3, when the vehicle speed in the cornering session, the front wheel steering angle of the vehicle with ST-SMC is within a considerably smaller range as compared to the vehicle with SMC. By using ST-SMC, the RSV is more stable at high speeds. Low friction coefficient circumstances make it easy to completely saturate the available frictional force. As depicted in the Figure 4, the required braking force is applied only through dynamic braking. Because of this, RSV with ST-SMC was proposed in order to minimize noise and jitter in the system. By utilizing ST-SMC, the jitter of slip rate is decreased by 80.3% compared to using SMC because of the exponential term. It can be seen that, compared with the RSV with SMC, the RSV with ST-SMC can minimize the jitter effect, thereby reducing the slip rate tracking error. As shown in Figures 5(a) and 5(b), both axial velocities, the *X*-axis and the *Y*-axis, exhibit a bit of a radical shift on the cornering region, ranging from 17 m/s to 15.2 m/s in Figure 5(a) and -0.38 m/s to -0.8 m/s in Figure 5(b). The results in Figure 5(a) also show that the velocity on the *X*-axis of the vehicle is far higher than the velocity on the *Y*-axis, indicating that the inertia cornering region on the *X*-axis of the vehicle is significantly higher. In the case of conventional braking, both the front and rear wheels are only subjected to torque braking. SMC and ST-SMC are shown side by side in Figure 6 to illustrate the differences in rear wheel slip rate. It can be observed that the slip of the RSV with SMC will cause disturbance during braking. When the vehicle's longitudinal speed hits its maximum, the regenerative braking is withdrawn for the drive wheels.
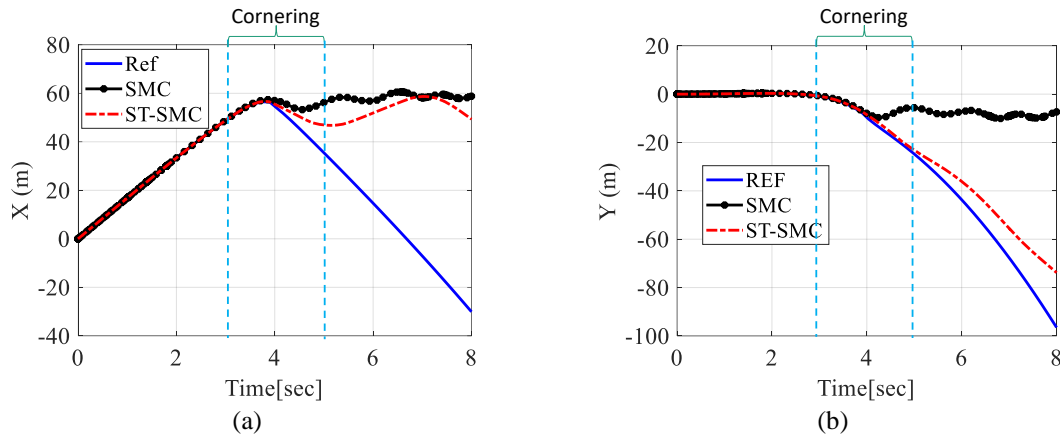
Figure 3. Sample of longitudinal and lateral error error for all session of simulations performances between proposed ST-SMC and SMC for the c-shape cornering (a) sample of longitudinal error performances for all session of simulations and (b) sample of lateral error performances for all session of simulations
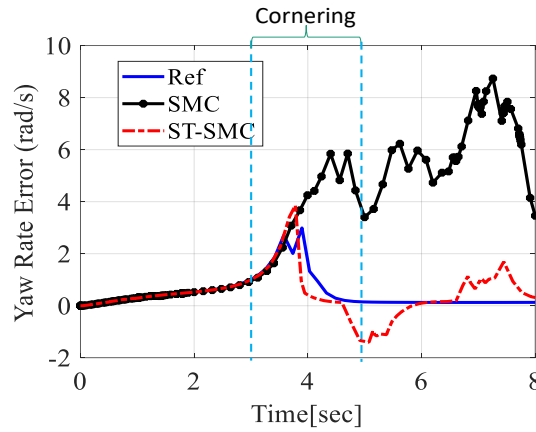


Figure 4. Yaw rate error performances between proposed ST-SMC and SMC for the c-shape cornering
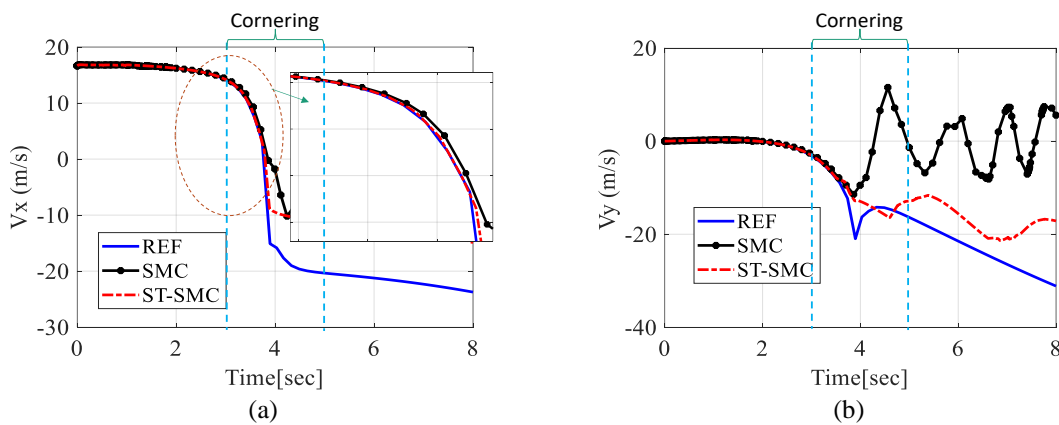


Figure 5. Sample of linear velocity performances for longitudinal motion and lateral motion (a) sample of linear velocity performances for the longitudinal motion for all session of simulations and (b) sample of linear velocity performances for the lateral motion of an RSV for all session of simulations
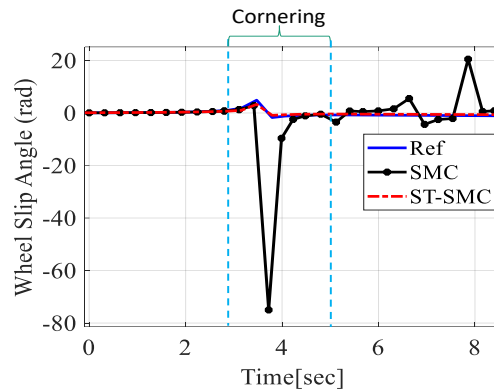
Figure 6. Sample of wheel slip angles performance between proposed ST-SMC and SMC for the c-shape cornering

## 5.   CONCLUSION

Steering angle of RSV controls through the proposed ST-SMC is presented, showing the proportional reducing with the positioning and velocities input shaping each axis motion of the vehicle. In terms of overall performance, the reduction of lateral and longitudinal velocities affects the vehicle steering and slip angle performances. The proposed control reduced vehicle speed to make the vehicle slower during the cornering session, which correlated to kinetic energy reducing. The proposed ST-SMC has the potential to be optimized using a suitable optimization technique in order to get an optimum performance especially on the cornering road.

## REFERENCES

[1]   Z. Yu, X. Huang, and J. Wang, "A least-squares regression based method for vehicle yaw moment of inertia estimation," in *2015 American Control Conference (ACC)*, 2015, pp. 5432-5437, doi: 10.1109/ACC.2015.7172189.

[2]   E. Hashemi, M. Jalali, A. Khajepour, A. Kasaiezadeh, and S. K. Chen, "Vehicle Stability Control: Model Predictive Approach and Combined-Slip Effect," *IEEE/ASME Transactions on Mechatronics,* vol. 25, no. 6, pp. 2789-2800, Dec. 2020, doi: 10.1109/TMECH.2020.2993792.

[3]   H. Xu, Y. Zhao, W. Pi, Q. Wang, F. Lin, and C. Zhang, "Integrated Control of Active Front Wheel Steering and Active Suspension Based on Differential Flatness and Nonlinear Disturbance Observer," *IEEE Transactions on Vehicular Technology,* vol. 71, no. 5, pp. 4813-4824, May 2022, doi: 10.1109/TVT.2022.3151252.

[4]   C. Zhou, X.-H. Liu, and F.-X. Xu, "Intervention criterion and control strategy of active front steering system for emergency rescue vehicle," *Mechanical Systems and Signal Processing,* vol. 148, p. 107160, Feb. 2021, doi: 10.1016/j.ymssp.2020.107160.

[5]   G. Wang, Y. Liu, S. Li, Y. Tian, N. Zhang, and G. Cui, "New Integrated Vehicle Stability Control of Active Front Steering and Electronic Stability Control Considering Tire Force Reserve Capability," in *IEEE Transactions on Vehicular Technology,* vol. 70, no. 3, pp. 2181-2195, March 2021, doi: 10.1109/TVT.2021.3056560.

[6]   M. Dalboni *et al.*, "Nonlinear Model Predictive Control for Integrated Energy-Efficient Torque-Vectoring and Anti-Roll Moment Distribution," in *IEEE/ASME Transactions on Mechatronics,* vol. 26, no. 3, pp. 1212-1224, June 2021, doi: 10.1109/TMECH.2021.3073476.

[7]   O. Nazarova, V. Osadchyy, and V. Brylystyi, "Research on the Influence of the Position of the Electric Vehicles Mass Center on Their Characteristics," in *2020 IEEE Problems of Automated Electrodrive. Theory and Practice (PAEP)*, 2020, pp. 1-4, doi: 10.1109/PAEP49887.2020.9240824.

[8]   N. M. Adam, A. Irawan, and F. K. Faudzi, "Impedance control on rack steering vehicle for inertia shaping on cornering track," *International Journal of Dynamics and Control,* vol. 7, no. 4, pp. 1434-1442, 2019, doi: 10.1007/s40435-018-0498-8.

[9]   X. Ma, P. K. Wong, J. Zhao, and Z. Xie, "Cornering stability control for vehicles with active front steering system using T-S fuzzy based sliding mode control strategy," *Mechanical Systems and Signal Processing,* vol. 125, pp. 347-364, June 2019, doi: 10.1016/j.ymssp.2018.05.059.

[10]  F. Zhang, J. Gonzales, S. E. Li, F. Borrelli, and K. Li, "Drift control for cornering maneuver of autonomous vehicles," *Mechatronics,* vol. 54, pp. 167-174, Oct. 2018, doi: 10.1016/j.mechatronics.2018.05.009.

[11]  L. A. Yekinni and A. Dan-Isa, "Fuzzy Logic Control of Goal-Seeking 2-Wheel Differential Mobile Robot Using Unicycle Approach," in *2019 IEEE International Conference on Automatic Control and Intelligent Systems (I2CACIS)*, pp. 300-304, 2019, doi: 10.1109/I2CACIS.2019.8825082.

[12]  M. Cui, "Observer-Based Adaptive Tracking Control of Wheeled Mobile Robots With Unknown Slipping Parameters," *IEEE Access,* vol. 7, pp. 169646-169655, 2019, doi: 10.1109/ACCESS.2019.2955887.

[13] R. Siegwart and I. R. Nourbakhsh, *Introduction to Autonomous Mobile Robots* in Bradford Book, 2004.
[14] V. Utkin, J. Guldner, and J. Shi, "Sliding Mode Control in Electro-Mechanical Systems" in *Boca Raton*, CRC Press, 2017, doi: 10.1201/9781420065619.
[15] C. Papachristos and A. Tzes, "Large object pushing via a direct longitudinally-actuated unmanned Tri-TiltRotor," in *21st Mediterranean Conference on Control and Automation*, 2013, pp. 173-178, doi: 10.1109/MED.2013.6608717.
[16] Z. Wang and D. Yin, "Design and Implementation of Vehicle Control System for Pure Electric Vehicle Based on AUTOSAR Standard," in *2019 22nd International Conference on Electrical Machines and Systems (ICEMS)*, 2019, pp. 1-5, doi: 10.1109/ICEMS.2019.8921856.
[17] L. Niu and L. Ye, "Adaptive Tracking Control of Nonlinear Systems Using Neural Networks," in *2009 International Asia Conference on Informatics in Control, Automation and Robotics*, 2009, pp. 12-15, doi: 10.1109/CAR.2009.15.
[18] M. Shuhua and L. Wei, "Non-linear PID control method with feed-forward in smart car," in *2009 Chinese Control and Decision Conference*, 2009, pp. 462-465, doi: 10.1109/CCDC.2009.5195008.
[19] Q. Yang, J. l. Zhou, and D. x. Gao, "Robust Optimal Sliding Mode Controller Design for Uncertain System with Composite Disturbances and Its Application to AUV," in *2021 33rd Chinese Control and Decision Conference (CCDC)*, 2021, pp. 5362-5367, doi: 10.1109/CCDC52312.2021.9602281.
[20] A. Titli, S. Roukieh, and E. Dayre, "Three control approaches for the design of car semi-active suspension (optimal control, variable structure control, fuzzy control)," in *Proceedings of 32nd IEEE Conference on Decision and Control*, vol. 3, pp. 2962-2963, 1993, doi: 10.1109/CDC.1993.325743.
[21] Z. Yan and D. Qingyu, "Design of adaptive fuzzy controller in air-cushioned headbox," in *2010 2nd International Asia Conference on Informatics in Control, Automation and Robotics (CAR 2010)*, 2010, vol. 3, pp. 9-12, doi: 10.1109/CAR.2010.5456736.
[22] M. I. P. Azahar, A. Irawan, and R. M. T. R. Ismail, "Self-tuning hybrid fuzzy sliding surface control for pneumatic servo system positioning," *Control Engineering Practice,* vol. 113, p. 104838, August 2021, doi: 10.1016/j.conengprac.2021.104838.
[23] L. Yang and J. Yang, "Nonsingular fast terminal sliding-mode control for nonlinear dynamical systems," *International Journal of Robust and Nonlinear Control,* vol. 21, no. 16, pp. 1865-1879, 2011, doi: 10.1002/rnc.1666.
[24] S. Yu, X. Yu, B. Shirinzadeh, and Z. Man, "Continuous finite-time control for robotic manipulators with terminal sliding mode," *Automatica,* vol. 41, no. 11, pp. 1957-1964, 2005/11/01/ 2005, doi: 10.1016/j.automatica.2005.07.001.
[25] J. Cao, C. Song, S. Peng, S. Song, X. Zhang, and F. Xiao, "Trajectory Tracking Control Algorithm for Autonomous Vehicle Considering Cornering Characteristics," *IEEE Access,* vol. 8, pp. 59470-59484, 2020, doi: 10.1109/ACCESS.2020.2982963.

## BIOGRAPHIES OF AUTHORS

**Norsharimie Mat Adam** received her master's degree in MSc. Robotic and System Control from Universiti Malaysia Pahang in 2018. Currently she is pursuing PhD degree at the Faculty of Electrical & Electronics Engineering Technology, Universiti Malaysia Pahang. Her research interests include modeling and control of linear systems, model order reduction, artificial intelligent systems, and applications of control theory. She can be contacted at email: sharimie.adam@gmail.com.

**Addie Irawan** is an Associate Professor at University Malaysia Pahang (UMP) and served with Faculty of Electrical and Electronics Engineering Technology (FTKEE), Universiti Malaysia Pahang (UMP), Malaysia since 2005. Principal in Robotics, Dynamics, Motion Control and Mechanism as well as Computer & Networks area specific in Network Protocols and ISP. He received a Doctor of Engineering degree in Artificial Systems Science (System Control and Robotics) from Chiba University, Japan in 2012; and received Master of Science in Computer Communication & Network from Universiti Sains Malaysia (USM) in 2005. He also a Professional Engineer (PEng) of the Board of Engineers Malaysia (BEM), Charted Engineer (CEng) and Charted Marine Engineer (CMarEng) under the British Engineering Council via Institute of Marine Engineering Science and Technology (IMarEST) as well as Senior Member of Institute of Electrical and Electronics Engineers (IEEE). He can be contacted at email: addieirawan@ump.edu.my.

**Mohd Ashraf Ahmad** received his first degree in B.Eng Electrical Mechatronics and Master Degree in M.Eng Mechatronics and Automatic Control from University of Technology Malaysia (UTM) in 2006 and 2008, respectively. In 2015, he received a Ph.D in Informatics (Systems Science) from Kyoto University. Currently, he is an Associate Professor in the Faculty of Electrical and Electronics Engineering Technology, University Malaysia Pahang (UMP). His current research interests are model-free control, control of mechatronic systems, nonlinear system identification and vibration control. He has been serving as Associate Editor for the International Journal of Electrical and Computer Engineering since 2016, Applications of Modelling and Simulation since 2017, and Journal of Future Robot Life since 2019. He can be contacted at email: mashraf@ump.edu.my.